arXiv:quant-ph/0410119v1 15 Oct 2004

Entanglement of large atomic samples: a Gaussian state analysis

Jacob Sherson and Klaus Mølmer
QUANTOP, Danish Research Foundation Center for Quantum Optics,
*Department of Physics and Astronomy, University of Aarhus, DK 8000 Aarhus C, Denmark**

We present a Gaussian state analysis of the entanglement generation between two macroscopic atomic ensembles due the continuous probing of collective spin variables by optical Faraday rotation. The evolution of the mean values and the variances of the atomic variables is determined and the entanglement is characterized by the Gaussian entanglement of formation (GEoF) and the logarithmic negativity. The effects of induced opposite Larmor rotation of the samples and of light absorption and atomic decay are analyzed in detail.

I. INTRODUCTION

Macroscopic samples of atoms as a resource of entanglement have attracted attention because of their robustness to single particle losses which leads to msec lifetimes of the entangled states and because of the effective coupling to light as needed for quantum repeaters and memories in quantum communication networks [1, 2]. The theoretical proposal [3, 4] surprisingly showed that by merely probing the state of atomic samples with light from a classical light source, one induces an atomic dynamics where the quantum state evolves by state reduction to entangled states. The experimental implementation of the proposal [3] led to the first demonstration of entanglement between macroscopic ($\sim 10^{12}$) numbers of atoms [5, 6]. In this work we extend the theoretical Heisenberg picture analysis in [3] with an analysis addressing directly the quantum state of the atoms and its time evolution due to the interaction with the continuous wave (cw) probe field, the back action of the measurements, obtained continuously in time, and light absorption and atomic decay. We note that a quantum trajectory approach with simulated state vector dynamics was presented in [7, 8] to provide a microscopic description of the dynamics, but because of the dimensions of the Hilbert spaces involved, these simulations were restricted to a few tens of atoms. We retain in this work the careful attention of [7, 8] to the quantum mechanical effects of the measurement in a treatment of macroscopic samples by a practically exact Gaussian Ansatz for the quantum states. This permits the use of the powerful formalism of correlation matrices for Gaussian states [9, 10].

The successful experimental verification of entanglement of macroscopic samples [5] utilizes Larmor rotation of the samples. This presents an experimental advantage compared to measuring on only one EPR quadrature at a time, but until now there has been no thorough theoretical examination of the precise effect of these rotations on the entanglement generation rate. We give explicit analytic expressions for the entanglement generation rate as a function of rotation frequency in the absence of light absorption and numerical results in the presence of light absorption and atomic decay.

In section II we introduce the description of the atomic and light variables and briefly discuss the basic interaction. In section III we introduce a Gaussian description of the interaction and solve a nonlinear differential equation for the atomic variables in the absence of light absorption. The entanglement is quantified in terms of the GEoF. In section IV we describe the effects of light absorption and we present analytic solutions for the atomic variables in the case of small decoherence effects and numerical solutions for the general case. In section V we discuss the evolution of the mean values of the atomic variables during the interaction. Section VI concludes the paper.

II. SETUP AND INTERACTION

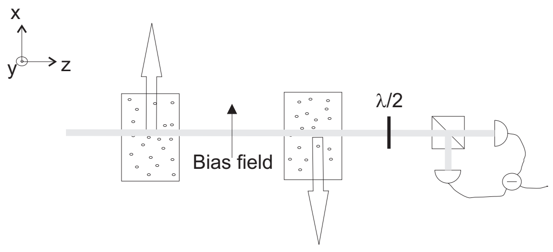

Figure 1: A continuous wave light beam linearly polarized along the x-axis is sent through two macroscopic samples of atoms optically pumped with collective spins in the positive and the negative x-direction respectively. The polarization rotation of the field is monitored continuously. A bias field along the x-direction is applied to induce Larmor rotation of the atomic spins in the y-z plane during the measurement.

We consider the system studied experimentally in [5, 6] and sketched in Fig. 1 with two macroscopic samples of spin 1/2 particles polarized along the positive and negative x-axis respectively. The samples interact with an off resonant linearly polarized light beam giving rise to a Kerr-interaction between the macroscopic spin operator, $\vec{J}$, and the Stokes operator of light, $\vec{S}$. We assume the two atomic samples to be prepared close to the maximally polarized state along x with magnitudes

---

*Electronic address: sherson@phys.au.dk,moelmer@phys.au.dk

$J_{x1} = J_x \equiv N_a/2$ and $J_{x2} = -J_x$, where N_a is the common number of atoms in each of the two samples. Here and in the remaining part of this paper we set $\hbar = 1$. For macroscopic samples of atoms the quantum mechanical uncertainty in J_x is negligible compared to the magnitude of J_x which can therefore be considered a classical number. With large number of photons in the probing beam the same argument applies to the Stokes vector component S_x. Defining a vector of observables

$$\mathbf{y} = \begin{pmatrix} x_{A1} \\ p_{A1} \\ x_{A2} \\ p_{A2} \\ x_L \\ p_L \end{pmatrix} = \begin{pmatrix} J_{y1}/\sqrt{J_x} \\ J_{z1}/\sqrt{J_x} \\ -J_{y2}/\sqrt{J_x} \\ J_{z2}/\sqrt{J_x} \\ S_y/\sqrt{S_x} \\ S_z/\sqrt{S_x} \end{pmatrix} \tag{1}$$

the system is described to a good approximation by operators which obey the usual position and momentum commutation relation $[x_i, x_j] = [p_i, p_j] = 0, [x_i, p_j] = i\delta_{ij}$. The Hamiltonian for the interaction between the light and either of the two samples will be given by an expression of the form $H_i = \kappa p_i p_L$. The coupling strength κ is proportional to the square root of the number of atoms and the square root of the photon number, and it will be related to other physical parameters in the numerical examples presented below.

To model the continuous interaction between the atoms and the incoming cw-light field we propose along the lines of [11] to split the light field into independent slices of duration τ. The interaction between the samples and each light segment are then treated one after the other. The continuous interaction and detection of the resulting field then corresponds to taking the $\tau \to 0$ limit.

Since both the number of photons and atoms are very large and the initial polarized state of the atoms and the light is a minimum uncertainty state, a Gaussian distribution function for the quantum variables is valid. This form is preserved both by the interaction and by the detection [9, 10] so we can use the powerful formalism of correlation matrices to describe the dynamical evolution of the system. Within the Gaussian approximation all information is contained in the first two moments of the quantum variables. We are interested in the entanglement properties of the samples which are not changed by local displacement operations so the second moments are of primary interest. These are collected in the 6x6 covariance matrix defined by $\gamma_{ij} = 2Re\,\langle (y_i - \langle y_i \rangle)(y_j - \langle y_j \rangle)\rangle$. Knowing how the covariance matrix is updated during the interaction and by the detection allows us to monitor the dynamics real-time.

III. NO LIGHT INDUCED DECOHERENCE

We model the evolution of the atomic system from t to $t + \tau$ by taking sequentially into account the interaction of initially coherent light with each atomic sample, the rotation of the samples, and the homodyne detection of the x_L quadrature of the light. The evolution of $\mathbf{y}$ in the Heisenberg picture due to the interaction between the light segment and samples 1(2) is given by $\mathbf{y}(t+\tau) = S_{1(2)}\mathbf{y}(t)$ with the interaction matrices:

$$S_1 = \begin{pmatrix} 1 & 0 & 0 & 0 & 0 & \kappa_\tau \\ 0 & 1 & 0 & 0 & 0 & 0 \\ 0 & 0 & 1 & 0 & 0 & 0 \\ 0 & 0 & 0 & 1 & 0 & 0 \\ 0 & \kappa_\tau & 0 & 0 & 1 & 0 \\ 0 & 0 & 0 & 0 & 0 & 1 \end{pmatrix} \qquad S_2 = \begin{pmatrix} 1 & 0 & 0 & 0 & 0 & 0 \\ 0 & 1 & 0 & 0 & 0 & 0 \\ 0 & 0 & 1 & 0 & 0 & \kappa_\tau \\ 0 & 0 & 0 & 1 & 0 & 0 \\ 0 & 0 & 0 & \kappa_\tau & 1 & 0 \\ 0 & 0 & 0 & 0 & 0 & 1 \end{pmatrix}$$

Taking into account also the Larmor precession and the detection, the correlation matrix will evolve according to:

$$\gamma(t+\tau) = M[R \cdot S_2 \cdot S_1 \cdot \gamma(t) \cdot S_1^T \cdot S_2^T \cdot R^T] \tag{2}$$

where R denotes a block diagonal matrix rotating the atomic variables of the samples an angle $\pm\omega\tau$ and leaving the light variables unchanged. M[...] denotes the effect of the homodyne detection. Let the covariance matrix before the homodyne measurement be given by:

$$\gamma = \begin{pmatrix} \gamma_a & \gamma_c \\ \gamma_c^T & \gamma_b \end{pmatrix} \tag{3}$$

where γ_a is a 4x4 matrix describing the atomic subsystem, and γ_b is a 2x2 matrix describing the light system. All atom-light correlations are contained in γ_c. After the detection the atomic part of the correlation matrix is then given by [9, 10]:

$$\gamma_a \to \gamma_a - \gamma_c(\pi\gamma_b\pi)^- \gamma_c^T \tag{4}$$

where $\pi = \mathrm{diag}(1,0)$ because one quadrature of the light is assumed to be detected perfectly and $(\,\cdot\,)^-$ denotes the Moore-Penrose pseudo-inverse of a matrix.

When Eq.(2) is evaluated for short time segments τ, the change in γ is quadratic in κ_τ. κ_τ^2 is proportional to the photon number in the beam segment, i.e. proportional to τ and rewriting $\kappa_\tau^2 = \tilde{\kappa}^2\tau$, the differential limit for the atomic correlation matrix can be formed:

$$\frac{d\gamma_a}{dt} = \mathbf{r}\gamma_a + \gamma_a\mathbf{r}^T + \tilde{\kappa}^2(\tilde{A} - \gamma_a\tilde{B}\gamma_a^T) \tag{5}$$

where:

$$\tilde{A} = \begin{pmatrix} 1 & 0 & 1 & 0 \\ 0 & 0 & 0 & 0 \\ 1 & 0 & 1 & 0 \\ 0 & 0 & 0 & 0 \end{pmatrix}, \quad \tilde{B} = \begin{pmatrix} 0 & 0 & 0 & 0 \\ 0 & 1 & 0 & 1 \\ 0 & 0 & 0 & 0 \\ 0 & 1 & 0 & 1 \end{pmatrix} \tag{6}$$

and

$$\mathbf{r} = \begin{pmatrix} 0 & \omega & 0 & 0 \\ -\omega & 0 & 0 & 0 \\ 0 & 0 & 0 & -\omega \\ 0 & 0 & \omega & 0 \end{pmatrix} \tag{7}$$

We note that the evolution of the atomic covariance matrix caused by the measurements given by Eq. (4) is deterministic (despite the random outcomes of the detection) and non-linear.

A. Ricatti equation and solution

The nonlinear differential Eq. (5) can be solved using the Ricatti method as eg. mentioned in the appendix of [12]. The generic Ricatti equation is:

$$\frac{d\mathbf{V}}{dt} = \mathbf{C} - \mathbf{D}\mathbf{V}(t) - \mathbf{V}(t)\mathbf{A} - \mathbf{V}(t)\mathbf{B}\mathbf{V}(t) \tag{8}$$

Using the decomposition $\mathbf{V}(t) = \mathbf{W}(t)\mathbf{U}^{-1}(t)$ it can be shown that the nonlinear differential equation can be replaced by the linear equation:

$$\begin{pmatrix} \frac{d\mathbf{W}(t)}{dt} \\ \frac{d\mathbf{U}(t)}{dt} \end{pmatrix} = \begin{pmatrix} -\mathbf{D} & \mathbf{C} \\ \mathbf{B} & \mathbf{A} \end{pmatrix} \begin{pmatrix} \mathbf{W}(t) \\ \mathbf{U}(t) \end{pmatrix} \tag{9}$$

Matching our equation to the generic Ricatti equation and observing that $\gamma_a^T = \gamma_a$ we obtain the linear set of equations

$$\begin{pmatrix} \frac{d\mathbf{W}(t)}{dt} \\ \frac{d\mathbf{U}(t)}{dt} \end{pmatrix} = \begin{pmatrix} \mathbf{r} & \tilde{\kappa}^2\tilde{\mathbf{A}} \\ \tilde{\kappa}^2\tilde{\mathbf{B}} & \mathbf{r} \end{pmatrix} \begin{pmatrix} \mathbf{W}(t) \\ \mathbf{U}(t) \end{pmatrix} \tag{10}$$

where we have used that $\mathbf{r} = -\mathbf{r}^T$.

Choosing the **W** and **U** matrices to start out as 4x4 identity matrices this system of coupled linear differential equations can be solved. The result is fairly complicated but can be simplified by applying a time dependent rotation of $\mp\omega t/2$ to sample one and two respectively. A further simplification can be made by noting that the measured quadratures are really the sum of p's and the difference of x'es. In the sum/difference basis:

$$\begin{pmatrix} 1 & 1 & 0 & 0 \\ 0 & 0 & 1 & 1 \\ 1 & -1 & 0 & 0 \\ 0 & 0 & 1 & -1 \end{pmatrix} \tag{11}$$

where the first and the third columns are the basis vectors corresponding to the sum of x'es and p's and the second and the fourth correspond to the difference, we get the sum/difference correlation matrix:

$$\gamma_a^{sd} = \begin{pmatrix} a_+ & 0 & 0 & 0 \\ 0 & \frac{1}{a_-} & 0 & 0 \\ 0 & 0 & \frac{1}{a_+} & 0 \\ 0 & 0 & 0 & a_- \end{pmatrix} \tag{12}$$

where $a_\pm = 1 + \tilde{\kappa}^2 t \pm \frac{\tilde{\kappa}^2}{\omega}\sin(\omega t)$. Defining the total accumulated interaction at time t as $\kappa_t^2 \equiv \tilde{\kappa}^2 t$ and the total rotated angle $\theta \equiv \omega t$ we get the main result of this section:

$$a_\pm = 1 + \kappa_t^2 \pm \frac{\kappa_t^2}{\theta}\sin(\theta) \rightarrow \begin{cases} 1 + \kappa_t^2 \pm \kappa_t^2 & \theta \rightarrow 0 \\ 1 + \kappa_t^2 & \theta \rightarrow \infty \end{cases} \tag{13}$$

We see that as $\theta \rightarrow 0$ we get $1 + 2\kappa_t^2$ and 1, i.e. the characteristic squeezing and anti-squeezing of the measured and their conjugate variables and no change in the unobserved ones. For $\theta \rightarrow \infty$, i.e. after many rotations we squeeze the two quadratures symmetrically and anti-squeeze their conjugate variables by the factor $1 + \kappa_t^2$. Note that the reduced squeezing by a factor of two in the rotated case comes from the fact that we effectively only spend half the time measuring on each quadrature. The result without rotations matches that of [3] and the strongly rotated result agrees with calculations from [6].

B. Gaussian Entanglement of Formation

As an entanglement measure we choose the recently proposed Gaussian Entanglement of Formation(GEoF) of [13]. This measure agrees with the Von Neuman entropy for pure states and it can easily be calculated from the covariance matrix. It is given by:

$$GEoF(\Delta) = c_+(\Delta)\log_2[c_+(\Delta)] - c_-(\Delta)\log_2[c_-(\Delta)] \tag{14}$$

where $c_\pm(\Delta) = (\Delta^{-1/2} \pm \Delta^{1/2})^2/4$ and $\Delta^2 = \mathrm{Var}(x_1 - x_2)\mathrm{Var}(p_1 + p_2)$. Note that the small Δ approximation:

$$GEoF(\Delta) \approx \log_2\left(\frac{1}{\Delta}\right) + \frac{1}{\ln 2} - 2 \tag{15}$$

shows an error of 10^{-5} at $\Delta = 1/100$, 0.001 at $\Delta = 1/10$, and only 1% at $\Delta = 1/5$ so it is widely applicable. From Eqs. (12) and (13) Δ^2 can be shown to be

$$\Delta^2 = \frac{1}{(1 + \kappa_t^2)^2 - \frac{\kappa_t^4}{\theta^2}\sin^2(\theta)} \tag{16}$$

which tells us that the entanglement will scale as $\log_2(\kappa_t^2) = 2\log_2(\kappa_t)$ with rotation and with $\log_2(\kappa_t)$ without rotations. The factor of two is exactly what one should expect since rotations enable us to squeeze both quadratures compared to squeezing only one of them. This effect was also observed in [7].

In Fig. 2 we show the entanglement plotted as a function of κ_t and θ. As can be seen, the transition from the static to the rotated regime occurs before one full revolution is reached. That is, given a total interaction time, t, there is no real gain in choosing the frequency larger than $\omega_{\text{crit}} = 1/t$. This arises from the fact that we measure $x_- \cos(\theta) + p_+ \sin(\theta)$ and this operator commutes with the operators measured at all previous times (other values of θ). It is therefore the accumulated measurement on each quadrature that counts and this will not benefit from many rotations compared to a single rotation. In the experiments of [5, 6] $\nu_L \approx 320$kHz and $T_{\text{probe}} \approx 1$ms so the spins will rotate several hundreds of times in one pulse and the results are thus firmly obtained in the ω independent regime. Note that both axes in Fig. 2 represent time dependent quantities.

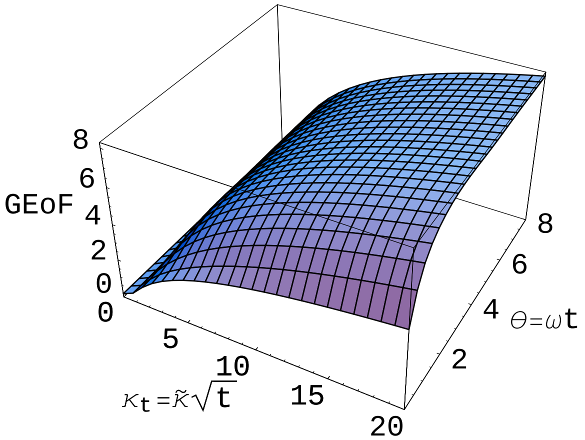

Figure 2: 3D plot of GEoF as a function of the accumulated interaction strength κ_t and the rotated angle θ. The plot clearly shows that the transition from the static to the rotated regime has occurred already before one full revolution of the atomic spins has taken place. In both the static and the rotated regions we clearly see the logarithmic behavior of the GEoF as a function of κ_t.

IV. LIGHT ABSORPTION AND ATOMIC DECAY

Due to the interaction with the light field every atom has a rate by which it is excited and decays by spontaneous emission to any of the atomic ground states, and every photon is absorbed with a given probability. This atomic depumping parameter and the photon absorption probability are given by $\eta_\tau \equiv \eta\tau = \Phi\tau\frac{\sigma}{A}\left(\frac{\Gamma}{\Delta}\right)^2$, and $\epsilon = N_a\frac{\sigma}{A}\left(\frac{\Gamma}{\Delta}\right)^2$ respectively. Φ is the photonic flux, A is the cross section of the atomic sample illuminated by the light, Δ is the detuning from resonance, σ is the cross section on resonance for the probed transition, and Γ is the corresponding spontaneous decay rate. The optical density on resonance is $\alpha_0 = N_a\frac{\sigma}{A}$. This gives the relation for the coupling parameter introduced above, $\kappa_\tau^2(0) = \eta_\tau\alpha_0$. The decay of the mean spin makes the coupling constant time dependent, $\kappa_\tau^2 = \kappa_\tau^2(0)e^{-\eta t}$. We will in our numerical simulations use the experimentally motivated values of 5 MHz for the decay rate Γ and 1000 MHz for the detuning Δ. Many results will be presented as a function of α_0 so a brief discussion of the experimentally realizable optical densities is in order. In the experiments of [5, 6] $\alpha_0 \approx 5$ whereas optical densities of 100 or more can be routinely achieved in MOTs (see e.g. [14]). Using a Bose-Einstein condensate $\alpha_0 \approx 1000$ can be achieved.

A. Covariance matrix update and Ricatti equation

We now derive an expression for the time evolution of the covariance matrix due to photon loss and atomic decay. Due to atomic decay, during a time interval τ, a fraction η_τ of the atoms decays into a random mixture of the ground states, giving rise to the new value of the variance of one of the atomic collective spin component:

$$\begin{aligned} < J_z'^2 > &= (1-\eta_\tau)^2 < J_z^2 > + (1-(1-\eta_\tau)^2)N/4 \\ &\approx (1-\eta_\tau)^2 < J_z^2 > + \eta_\tau N/4 + \eta_\tau N/4 \end{aligned} \quad (17)$$

in the $\eta_\tau \ll 1$ limit. The atomic decay leads to a corresponding reduction of the mean spin $J_x' = (1-\eta_\tau)J_x$.

At this stage the gas contains two components: the atoms which have not decayed, described by the first two terms in the latter expression and the ones which have decayed, described by the last term. If nothing else happens to the atoms, subsequent interaction with the light can have no further effect on the random component, but a new fraction of atoms will be randomized and we obtain the iterated expression for the spin variance

$$\begin{aligned} < J_{z,1}^2 > &= (1-\eta_\tau)^2 < J_{z,0}^2 > + \eta_\tau\frac{N}{4} + \eta_\tau\frac{N}{4} \\ < J_{z,2}^2 > &= (1-\eta_\tau)^2[(1-\eta_\tau)^2 < J_{z,0}^2 > + \eta_\tau\frac{N}{4}] \\ &\quad + \eta_\tau\frac{N(1-\eta_\tau)}{4} + \eta_\tau[1+(1-\eta_\tau)]\frac{N}{4} \\ ... &= ... \\ < J_{z,n}^2 > &= (1-\eta)^{2n} < J_{z,0}^2 > \\ &\quad + \eta_\tau\left[(1-\eta_\tau)^{n-1} + \sum_{j=n}^{2(n-1)}(1-\eta_\tau)^j\right]\frac{N}{4} \\ &\quad + \eta_\tau\sum_{j=0}^{n-1}(1-\eta_\tau)^j\frac{N}{4}. \end{aligned} \quad (18)$$

In the limit $n \to \infty$ only the last term, representing the fully random component of the gas, will contribute. The geometrical series gives $1/\eta_\tau$, so we see that the initial squeezing will decay exponentially as expected and we will end up with N unpolarized atoms each contributing 1/4 to the variance as expected. Note that in the spin 1/2 case this coincides with the noise of atoms in the coherent spin state in which the atomic samples are initialized in this paper. This does not, however, hold for higher spin.

Taking into account that the covariance matrix deals with the transverse spin components scaled by the macroscopic longitudinal mean spin, we obtain for the corresponding diagonal covariance matrix element:

$$\gamma_{a,ii}^n = (1-\eta_\tau)^n\gamma_{a,ii}^0 + \frac{\eta_\tau}{2}\left[\frac{1}{1-\eta_\tau} + \sum_{j=-n}^{n-2}(1-\eta_\tau)^j\right]. \quad (19)$$

This analysis treats the atoms that have decayed and the ones that have not decayed on unequal footing, and it hence breaks with the Gaussian state Ansatz, which assumes that all information is in the collective variance and mean values for the entire atomic ensemble. The analysis does not make it easy to treat the coherent part of the interactions and the measurement back action, that we are interested in, and we hence wish to investigate, whether restoration to the Gaussian state Ansatz will yield a large discrepancy with the exact results. To this end, we go back to the update formula, Eq. (17), and insist that the variance obtained here should be treated as the variance describing a Gaussian state ensemble, i.e., we do not discriminate between the two kinds of atoms. In subsequent time steps, we thus simply iterate the same expression, as if all atoms contribute evenly to the joint variance. The result of this iteration is readily obtained:

$$\gamma_a(t+\tau) = (1-\eta_\tau)\gamma_a(t) + \frac{N_a}{4J_x(t+\tau)}\eta_\tau \mathbf{I_4}. \qquad (20)$$

Note that since $J_x(t) = (N_a/2)e^{-\eta t}$ the last term will diverge exponentially in time. In order to compare with Eq. (19) we iterate the diagonal elements of Eq. (20) n times:

$$\gamma^n_{a,ii} = (1-\eta_\tau)^n \gamma^0_{a,ii} + \eta_\tau \sum_{j=1}^{n} (1-\eta_\tau)^{n-2j}. \qquad (21)$$

In the continuous limit $t = n\tau$ with $\eta\tau \to 0$ and $n \to \infty$ both Eq. (19) and Eq. (21) yield the same behavior:

$$\gamma_{a,ii}(t) = e^{-\eta t}\gamma_{a,ii}(t=0) + \sinh(\eta t) \qquad (22)$$

This supports the use of the update formula, Eq. (20), with the underlying assumption of a Gaussian state, together with the evolution of γ due to interaction and measurements. This approach was also utilized in [11, 15] albeit not with the careful justification presented above.

When light absorption is included the interaction of a light segment with one sample i is described by [15]:

$$\begin{aligned}\gamma(t+\tau) &= \bar{D}(\eta_\tau,\epsilon) S_i(\kappa_\tau)\gamma(t) S_i(\kappa_\tau)^T \bar{D}(\eta_\tau,\epsilon) \\ &\quad + D_i(\eta_\tau,\epsilon)\gamma_{\mathrm{noise},i} \qquad (23)\end{aligned}$$

where, following the above argument, for the first sample we have, $D_1(\eta_1,\epsilon_1) = \mathrm{diag}(\eta_1,\eta_1,0,0,\epsilon_1,\epsilon_1)$, $\bar{D}_1(\eta_1,\epsilon_1) = \sqrt{1-D_1(\eta_1,\epsilon_1)}$ and $\gamma_{\mathrm{noise},1} = \mathrm{diag}(\xi,\xi,0,0,1,1)$ (and similarly $D_2(\eta_2,\epsilon_2) = \mathrm{diag}(0,0,\eta_2,\eta_2,\epsilon_2,\epsilon_2)$, $\gamma_{\mathrm{noise},2} = \mathrm{diag}(0,0,\xi,\xi,1,1)$). The factor $\xi \equiv N_{at}/\langle J_x(t)\rangle$ starts out as 2 and increases exponentially because of the decay of the mean spin due to excitation and subsequent decay of atoms.

As in section III the differential equation for the correlation matrix can be found:

$$\frac{d\gamma_a}{dt} = \tilde{\mathbf{r}}\gamma + \gamma\tilde{\mathbf{r}}^T + \tilde{A} - (1-\epsilon)\tilde{\kappa}^2\gamma\tilde{B}\gamma^T \qquad (24)$$

where

$$\tilde{A} = \begin{pmatrix} \tilde{\kappa}^2 + \xi(t)\eta & 0 & \tilde{\kappa}^2\sqrt{1-\epsilon} & 0 \\ 0 & \xi(t)\eta & 0 & 0 \\ \tilde{\kappa}^2\sqrt{1-\epsilon} & 0 & \tilde{\kappa}^2 + \xi(t)\eta & 0 \\ 0 & 0 & 0 & \xi(t)\eta \end{pmatrix} \qquad (25)$$

$$\tilde{B} = \begin{pmatrix} 0 & 0 & 0 & 0 \\ 0 & 1-\epsilon & 0 & \sqrt{1-\epsilon} \\ 0 & 0 & 0 & 0 \\ 0 & \sqrt{1-\epsilon} & 0 & 1 \end{pmatrix} \qquad (26)$$

and $\tilde{\mathbf{r}} = \mathbf{r} - (\eta/2)\mathbf{I_4}$, where $\mathbf{r}$ is defined in Eq. (7). Note that the coefficients are now time dependent which complicates matters slightly.

This Ricatti equation can of course easily be solved numerically but is in its most general form too complicated to admit analytical solution. If noise terms arising from the absorption of light, i.e. all terms involving ϵ are neglected, the Ricatti equation can be solved without rotations and in the strongly rotated regime. These solutions will be derived first and then the general results will be discussed.

B. Analytical results

1. *Without rotations*

Without rotations γ_a becomes diagonal in the sum/difference basis if we neglect the photon absorption ($\epsilon = 0$). The two components involved in the measurement give:

$$\gamma^{sd}_{11} = \mathrm{Var}(x_{A1} + x_{A2}) = e^{-\eta t}[e^{2\eta t} + 2\alpha_0\eta t] \qquad (27)$$

$$\begin{aligned}\gamma^{sd}_{33} &= \mathrm{Var}(p_{A1} + p_{A2}) \\ &= \frac{e^{\eta t}\ (\delta\cosh(\delta\eta t) + \sinh(\delta\eta t))}{\delta\cosh(\delta\eta t) + (1+2\,\alpha_0)\ \sinh(\delta\eta t)} \qquad (28)\end{aligned}$$

where $\delta = \sqrt{1+4\alpha_0}$. The two remaining components increase exponentially:

$$\gamma^{sd}_{22} = \mathrm{Var}(x_{A1} - x_{A2}) = \gamma^{sd}_{44} = \mathrm{Var}(p_{A1} - p_{A2}) = e^{\eta t} \qquad (29)$$

The validity of this solution can be tested by comparing with full numerical solutions. In Fig. 3 we plot the GEoF as a function of κ_t^2 (proportional with the total number of transmitted photons) and we see that in the case of dissipation, the entanglement reaches a maximum, and hereafter it decays and vanishes at a point when - because of the decay of the macroscopic spin - the atomic samples are in a mixed state with too few correlations to display actual entanglement.

As can be seen in Fig. 3 the analytic expression fits very well with the nontrivial result of the numerical calculation. The comparison is made for an optical depth, $\alpha_0 = 100$, corresponding to $\epsilon = \frac{\Gamma^2}{\Delta^2}\cdot\alpha_0 = 0.0025 \ll 1$. For larger optical depths, the quality of the analytical expression deteriorates whereas for lower optical densities the error of the analytical expression is negligible. This thus establishes the regime of validity for the analytic expression.

It is interesting to investigate when the maximum entanglement is reached and at what level as a function of

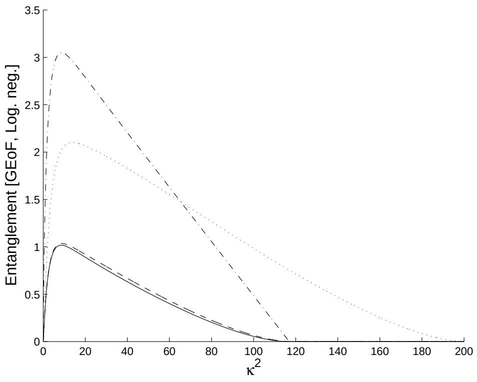

Figure 3: The generated entanglement vs. time of numerical simulation (full) and analytical solution(dashed). The optical density is 100 giving rise to only a slight difference between the two curves. The numerical solution is also represented in terms of the logarithmic negativity (dash-dot) which will be discussed in a later section. For further comparison a numerical simulation of GEoF with rotations ($\theta_{\text{total}} = 100 \cdot 2\pi$) is included (dotted).

α_0 and η. By differentiating $\Delta = \sqrt{\gamma_{22}\gamma_{33}}$ with respect to time we get:

$$t_{\text{crit}} = \frac{\operatorname{arccosh}(\frac{1}{2}\sqrt{\frac{-2\,\alpha^2 - 4\,\alpha^3 + (1+5\,\alpha+4\,\alpha^2)\sqrt{\alpha^3}}{\alpha^3}})}{\sqrt{1+4\,\alpha}\,\eta} \tag{30}$$

Note the simple inverse scaling with η. Since η and t only appear as a product in Eqs. (27) and (29) the inverse scaling of t_{crit} with η means that the maximum achievable entanglement will be independent of η. This behavior could also be predicted from the fact that as seen in Eqs. (28) and (29) Δ is a function of the product ηt.

2. Many rotations

To solve Eq. (24) in the case of many rotations we define a new set of canonical operators [6]:

$$\begin{array}{ll} \hat{x}_A = \frac{\hat{J}'_{y1} - \hat{J}'_{y2}}{\sqrt{2J_x}}, & \hat{x}_L = \sqrt{\frac{2}{S_x T}} \int_0^T \hat{S}_y(t)\cos(\omega_L t)dt \\ \hat{p}_A = \frac{\hat{J}'_{z1} + \hat{J}'_{z2}}{\sqrt{2J_x}}, & \hat{p}_L = \sqrt{\frac{2}{S_x T}} \int_0^T \hat{S}_z(t)\cos(\omega_L t)dt \end{array} \tag{31}$$

where $\hat{J}'_k$ refers to rotating frame coordinates, i.e. coordinates rotated an angle $\omega_L t$ compared to the usual lab frame coordinates. With these collective operators we regain the same formal description of the interaction as in the non-rotating case:

$$\begin{array}{ll} \hat{x}_A^{\text{out}} = \hat{x}_A^{\text{in}} + \kappa \hat{p}_L^{\text{in}}, & \hat{p}_A^{\text{out}} = \hat{p}_A^{\text{in}} \\ \hat{x}_L^{\text{out}} = \hat{x}_L^{\text{in}} + \kappa \hat{p}_A^{\text{in}}, & \hat{p}_L^{\text{out}} = \hat{p}_L^{\text{in}} \end{array} \tag{32}$$

Note that in this formalism the atomic correlation matrix is reduced to a 2x2 matrix whereas the correlation matrix of light remains a 2x2 matrix.

To illustrate the use of this new description first neglect all decoherence. With the usual update equation for the system we can form the differential equation for the atomic correlation matrix:

$$\frac{\partial \gamma_a}{\partial t} = \kappa^2 \begin{pmatrix} 1 & 0 \\ 0 & 0 \end{pmatrix} - \kappa^2 \gamma_a \begin{pmatrix} 0 & 0 \\ 0 & 1 \end{pmatrix} \gamma_a \tag{33}$$

When this is inserted into the Ricatti equation we easily derive the solution:

$$\gamma_a(t) = \begin{pmatrix} 1+\kappa_t^2 & 0 \\ 0 & \frac{1}{1+\kappa_t^2} \end{pmatrix} \tag{34}$$

which coincides with the rotated solution found in (13).

In order to treat decoherence analytically an approximation similar to that of section IV B 1, i.e. ignoring all ϵ dependent noise contributions, has to be made. The loss of light in the first sample, represented by ϵ will create asymmetries between the two samples which would cause the $\hat{x}_A$, $\hat{p}_A$ formalism of Eqs. (31,32) to break down. The regime of validity is thus expected to be similar to that of section IV B 1, i.e. $\alpha_0 \lesssim 100$.

We will consider the case of small values of ηt, i.e. the atomic samples retain a constant polarization along the x-axis and the differential equation has constant coefficients.

$$\gamma_a = \begin{pmatrix} e^{-\eta t}\left[(\alpha_0+4)(e^{\eta t}-1)+1\right] & 0 \\ 0 & \frac{7(e^{\eta t\beta}-1)+(e^{\eta t\beta}+1)\beta}{(e^{\eta t\beta}-1)(1+2\alpha_0)+(e^{\eta t\beta}+1)\beta} \end{pmatrix} \tag{35}$$

where $\beta = \sqrt{1+16\alpha_0}$.

An expansion in small ηt yields:

$$\gamma_{11} \approx (1-\eta t)(1+(\alpha_0+4)\eta t) \tag{36}$$

$$\gamma_{22} \approx \frac{2+\eta t(7+\sqrt{1+16\alpha_0})}{2+\eta t(1+2\alpha_0+\sqrt{1+16\alpha_0})} \tag{37}$$

Eq. (37) shows that a value of $1+2\alpha_0 > 7$, is required in order to get squeezing in p_A. Again we see that the variances are only functions of the two variables α_0 and ηt, and in the limit of vanishing noise we obtain $\gamma_{11} \to 1+\kappa_t^2$ and $\gamma_{22} \to 1/(1+\kappa_t^2)$, in accordance with our earlier results.

C. General results

We now turn to general numerical results beyond the regime of validity of the analytical solutions. First however we need to note that the GEoF is not applicable in the presence of the large asymmetries between the two cells that occurs at high α_0. We therefore introduce the logarithmic negativity of [16].

1. Logarithmic negativity

In this measure the symplectic spectrum of the partial transpose of the covariance matrix γ^{T_A} is used to cal-

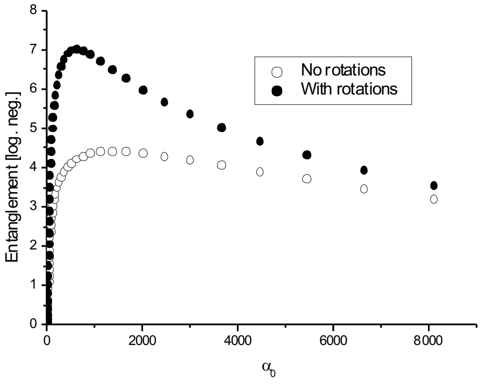

Figure 4: The maximum generated degree of entanglement as a function of α_0 with and without rotations.

culate the degree of entanglement. In the partial transposition all covariance matrix elements involving p_A and other observables are multiplied by (-1). The symplectic eigenvalues are most conveniently calculated by computing the eigenvalues of the matrix $\sigma^{-1}\gamma$, where σ is the matrix specifying the commutators: $\sigma_{\alpha\beta} = -i[y_\alpha, y_\beta]$. For m systems this gives 2m complex eigenvalues λ_k. The logarithmic negativity entanglement measure is then given by:

$$\text{log.neg.} = -\sum_{k=1}^{2m} \log_2[\min(1, 2|\lambda_k|)] \tag{38}$$

This is a valid entanglement monotone even for asymmetric samples but it does not coincide with the Von Neuman entropy for pure states as the GEoF does. If γ is diagonal in the sum/difference basis the eigenvalues can be expressed in terms of the diagonal entries:

$$\lambda = \pm i\sqrt{\frac{\gamma_{11}^{sd}\gamma_{44}^{sd} + \gamma_{22}^{sd}\gamma_{33}^{sd} \pm (\gamma_{11}^{sd}\gamma_{44}^{sd} - \gamma_{22}^{sd}\gamma_{33}^{sd})}{8}} \tag{39}$$

Without losses the covariances are specified by Eq. (13) giving a logarithmic negativity of $\log_2(\kappa_t^2) + 1$ and $2\log_2(\kappa_t^2)$ in the non-rotated and the rotated regimes respectively at $\kappa_t^2 \gg 1$. This is about a factor of two larger than the GEoF as specified in Eq. (15). The difference between GEoF and the logarithmic negativity in the presence of decoherence is illustrated in Fig. 3 where log. neg.(dash-dotted) is seen to be approximately a factor of three larger than the GEoF (full drawn).

2. Numerical results

In Fig. 4 we see the degree of entanglement generated with and without rotations. For low optical densities the improvement in the degree of entanglement due to rotations of the samples is close to the factor of two, which we got in the absence of decoherence. This is also illustrated in Fig. 3 for the case of $\alpha_0 = 100$. For higher optical densities the benefits of rotations seem to decrease. This is probably the result of the complicated interplay between the beneficial rotations and the increasing asymmetry between the two samples at high optical densities. It would certainly be a of great interest to study this further and to consider protocols where the samples are illuminated with lasers from both sides to restore their symmetry.

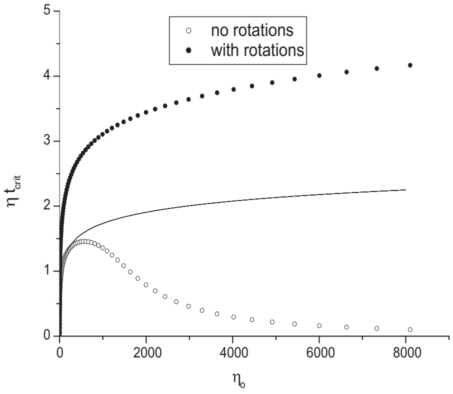

Figure 5: The ηt at which the entanglement has decayed to zero with and without rotations. The solid curve is calculated from Eqs. (27-29) assuming no rotations and no asymmetry between the two samples.

In Fig. 5 we show at which accumulated ηt the entanglement has decreased to zero. The theoretical curve is calculated from Eqs. (27) to (29). This solution fits the numerical results perfectly within the regime of validity, that is up to $\alpha = 200$. After this point entanglement decays rapidly, indicating that light losses which introduce asymmetry between the two samples are detrimental to the entanglement. As can be seen, the entanglement is not only increased by rotations. The rotated samples also seem to be a lot less vulnerable to light losses. Note that the decay in all cases happens in the vicinity of $\eta t = 1$ which could be expected from the exponential character of the decay of the mean spin and the resulting exponential growth of γ_{noise}.

V. MEAN VALUES

The generated entanglement is of no practical use unless the mean values of the atomic parameters are known. These will be affected by the interaction according to:

$$\langle \mathbf{y}(t+\tau)\rangle = \bar{D}_2 S_2 \bar{D}_1 S_1 \langle \mathbf{y}(t)\rangle \tag{40}$$

The mean values of the atomic variables after the interaction $\langle \mathbf{y_a}(\mathbf{t}+\tau)\rangle$ will subsequently transform according to the result of the homodyne measurement as:

$$\langle \mathbf{y}_a(t+\tau)\rangle \rightarrow \langle \mathbf{y}_a(t)\rangle + \gamma_c(\pi\gamma_b\pi)^{-1}(\chi, 0)^T \tag{41}$$

where χ is the difference between the measurement result and the mean value of the detected field component. That is, the evolution of the mean values is determined by the value of the correlation matrix at a given time.

Note also that it is the deviation from the mean value of the light that determines the evolution of the atomic mean values and not the measurement result itself. This will be discussed further below. The correlation matrix can be made diagonal in the sum/difference basis. We can therefore without loss of generality assume $\gamma_a(t)$ to be diagonal.

Having established the relatively large domain of validity of the analytical solution of the lossy system without rotations and negligible absorption losses in section IV B 1 we now apply the results of that section to Eq. (41). Given the fact that all mean values start out as zero we obtain the transformation of the atomic variables:

$$\langle \mathbf{y}_a(t+\tau)\rangle = (1-\eta_\tau/2)\langle \mathbf{y}_a(t)\rangle + \kappa_\tau \gamma_{33}^{sd} \begin{bmatrix} 0 \\ 1 \\ 0 \\ 1 \end{bmatrix} \chi \tag{42}$$

where γ_{33}^{sd} has the value specified in Eq. (28). We see that the two x-variables will have zero mean at all times and the two p-variables will experience the same evolution.

After the interaction we get in the limit of vanishing ϵ:

$$\gamma_{55} = 2\mathrm{Var}(x_L) = 1 + 2\gamma_{33}^{sd}\kappa_\tau^2 \tag{43}$$

Since we always work in the regime $\kappa_\tau^2 \ll 1$ and $\gamma_{33}^{sd} \approx 1$ in the relevant regime we can safely assume $\gamma_{55} = 1$. This means that the difference between the result of the homodyne measurement of x_L and its expectation value, will be a Gaussian random variable, χ with zero mean and variance 1/2.

Eq. (42) can be transformed into a stochastic differential equation with the solution:

$$\langle p(T)\rangle = \int_0^T e^{-\eta(T-t)/2}\frac{\tilde{\kappa}}{\sqrt{2}}\gamma_{33}^{sd} dW \tag{44}$$

where $dW = \sqrt{2dt}\chi$ is a stochastic Wiener increment with zero mean and variance dt. We recognize an exponential memory decay for early detection events, with $t_{mem} \approx 2/\eta$, and a covariance matrix weight factor, $\gamma_{33}^{sd}(t)$, based on the state of the atoms at the particular time. From Eq (44) it follows that the conditional mean value of p will be a stochastic variable with zero mean and variance:

$$\mathrm{Var}(\langle p(T)\rangle) = \frac{\tilde{\kappa}^2}{2}\int_0^T e^{-\eta(T-t)}(\gamma_{33}^{sd})^2 dt \tag{45}$$

To illustrate the physical interpretation of Eq. (45) we neglect decoherence and rotations. In this simple case we can perform the integration in Eq. (45) analytically:

$$\mathrm{Var}(\langle p(T)\rangle) = \frac{\tilde{\kappa}^2}{2}\int_0^T \frac{1}{(1+2\tilde{\kappa}^2 t)^2}dt = \frac{1}{2}\frac{\tilde{\kappa}^2 T}{1+2\tilde{\kappa}^2 T} \tag{46}$$

Since $\langle p_1(T)\rangle = \langle p_2(T)\rangle$, $\mathrm{Var}(\langle p_1(T)\rangle + \langle p_2(T)\rangle)$ will be four times the result of Eq. (46). It follows that at any time

$$\gamma_{33}^{sd} + 4\mathrm{Var}(\langle p\rangle) = \frac{1}{1+2\kappa_t^2} + \frac{2\kappa_t^2}{1+2\kappa_t^2} = 1 \tag{47}$$

Initially, the expectation value is well determined (0) whereas the quantum deviation from this value is given by the initial Gaussian distribution. After a significant interaction time the quantum mechanical uncertainty will be reduced but the value within the initial distribution at which the expectation value settles is uncertain.

Eqs. (42,44) express the conditional mean value of the atomic variable in terms of the difference between the optical read-out and its expectation value. It is interesting to obtain similar expressions in terms of the actual read-out. Since the coherent light initially has zero mean Eq. (40) shows us that the measured light component will have the mean value:

$$\langle x_L(t)\rangle = \kappa_\tau(\langle p_1(t)\rangle + \langle p_2(t)\rangle) \tag{48}$$

in the absence of ϵ decay. We thus start by writing χ in Eq. (42) as $\tilde{\chi} - 2\kappa_\tau\langle p(t)\rangle$. The atomic p variable thus changes as

$$\langle p(t+\tau)\rangle = (1-\eta_\tau/2)\langle p(t)\rangle + \kappa_\tau\gamma_{33}^{sd}(t)(\tilde{\chi} - 2\kappa_\tau\langle p(t)\rangle) \tag{49}$$

where $\tilde{\chi}$ is the random detector output. Taking the limit of inifitesimal $\tau = dt$ and defining the measured Wiener increment $d\tilde{W} = \sqrt{2dt}\tilde{\chi}$, we can integrate Eq. (49):

$$\langle p(T)\rangle = \int_0^T e^{-\eta(T-t)/2-\int_t^T 2\tilde{\kappa}^2\gamma_{33}^{sd}(t')dt'}\frac{\tilde{\kappa}}{\sqrt{2}}\gamma_{33}^{sd}(t)d\tilde{W} \tag{50}$$

In the limit of $\eta = 0$, $\gamma_{33}^{sd}(t) = 1/(1+2\tilde{\kappa}^2 t)$, and we can explicitly integrate the argument of the exponential function in Eq. (50), and we obtain

$$\begin{aligned}\langle p(T)\rangle &= \int_0^T \frac{1+2\tilde{\kappa}^2 t}{1+2\tilde{\kappa}^2 T}\frac{\tilde{\kappa}}{\sqrt{2}}\gamma_{33}^{sd} d\tilde{W} \\ &= \frac{\tilde{\kappa}}{\sqrt{2}(1+2\tilde{\kappa}^2 T)}\int_0^T d\tilde{W}\end{aligned} \tag{51}$$

This remarkable result shows that all measurements should be weighted equally in the absence of decoherence and rotations. When transformed back into regular angular momenta the common weight factor has a clear interpretation as the ratio between the shot to shot atomic noise contribution, the so-called projection noise, and the total noise in complete accordance with the result obtained in [6].

We stress that the result (51) was obtained for the non-rotated and non-decaying atomic systems. Decay can be included easily according to Eq. (50). In addition to the exponential damping term, this will involve a more complicated expression for $\gamma_{33}(t)$, and the conditioned mean value of p(T) will no longer be given by the integrated measurement outcome. We can understand that atomic mean values attained early during the measurements decay and hence they contribute less to the final $\langle p(T)\rangle$ than the most recent contributions to the optical detection. Since decay is inevitable, our analysis suggests that experiments must be carried out so that the optical signal is recorded in time bins which are much shorter than the atomic decoherence time η^{-1}. The results will then be in good agreement with our continuous update theory.

VI. CONCLUSION

In conclusion, we have presented a theory for the preparation of entangled atomic ensembles by detection of the Faraday polarization rotation of a continuous optical field passing though both ensembles. Our Gaussian Ansatz is very well justified for large atomic ensembles and for free space atom-light interaction, where only the interaction with many photons appreciably modifies the atomic state. The theory incorporates the interaction between the atoms and the optical field, atomic decay, and the measurement induced transformation of the atomic state. The reduction of the full quantum state description to a simple Gaussian state fully represented by a set of mean values and a covariance matrix makes the system straight forward to deal with numerically, and analytical results can be obtained in several important cases.

The entanglement between the atomic ensembles is quantified by the Gaussian Entanglement of Formation and the Logarithmic Negativity, and we identify the optimal performance of the entanglement scheme in the presence of atomic decay. Our analysis confirms a number of results, derived in less complete or purely numerical studies, and it presents an intuitive physical picture of the continuous transformation of the atomic quantum state from an initial state with no atomic correlations into a state with stronger correlations of the quantum observables, around mean values with a broader random distribution - but known by the experimentalist in every implementation of the experiment.

The results of our analysis are relevant for current experimental efforts to exploit entangled atomic ensembles for quantum purposes, but we also wish to emphasize the strengths of the theoretical method, which make it readily adapt to a wide variety of experiments.

Acknowledgments

Discussions with Lars Bojer Madsen, Eugene Polzik, Brian Julsgaard, Jörg Helge Müller, and Anders Sørensen are gratefully acknowledged

---

[1] C. W. Chou, S. V. Polyakov, A. Kuzmich, and H. J. Kimble, Phys. Rev. Lett. (2004).

[2] B. Julsgaard, J. Sherson, J. Cirac, J. Fiurasek, and E. Polzik, quant-ph/0410072 (2004).

[3] L. M. Duan, J. I. Cirac, P. Zoller, and E. S. Polzik, Phys. Rev. Lett. **85**, 5643 (2000).

[4] A. Kuzmich, L. Mandel, and N. P. Bigelow, Phys. Rev. Lett. **85**, 1594 (2000).

[5] B. Julsgaard, A. Kozhekin, and E. S. Polzik, Nature **413**, 400 (2001).

[6] J. Sherson, B. Julsgaard, and E. S. Polzik, quant-ph/0408146 (2004).

[7] A. DiLisi and K. Mølmer, Phys. Rev. A **66**, 032316 (2002).

[8] A. DiLisi, S. D. Siena, and F. Illuminati, Phys. Rev. A **70**, 012301 (2004).

[9] J. Eisert and M. B. Plenio, Int. J. Quant. Inf. **1**, 479 (2003).

[10] G. Giedke and J. I. Cirac, Phys. Rev. A **66**, 032316 (2003).

[11] K. Mølmer and L. B. Madsen, quant-ph/0402169 (2004).

[12] J. K. Stockton, J. M. Geremia, A. C. Doherty., and H. Mabuchi, Phys. Rev. A **69**, 032109 (2003).

[13] G. Giedke, M. M. Wolf, O. Kruger, R. F. Werner, and J. I. Cirac, Phys. Rev. Lett. **91**, 107901 (2003).

[14] W. Ketterle, K. B. Davis, M. A. Joffe, A. Martin, and D. E. Pritchard, Phys. Rev. Lett. **70**, 2253 (1993).

[15] K. Hammerer, K. Mølmer, E. S. Polzik, and J. I. Cirac (2003), quant-ph/0312156.

[16] K. Audenaert, J. Eisert, M. B. Plenio, and R. F. Werner, Phys. Rev. A **66**, 042327 (2002).